Amorphous CoFePO$_x$ Hollow Nanocube decorated with g-C$_3$N$_4$ quantum dots to Implement Efficient electrocatalytic performance for Oxygen Evolution Reaction

*Ke Yuan [a], Wei Zhou [a], Xiaoyan Zhu [a], Minzhe Chen [a], Chuheng Zhu [a], Ningning Chen [a], Haofeng Zuo [a], Aocheng Wang [a], Dengke Zhao[b, *], Maozhong An [c, d,*], Ligui Li [a *]*

a. New Energy Research Institute, College of Environment and Energy, South China University of Technology, Guangzhou 510006, China.

b. School of Materials Science and Engineering, Henan Normal University, Xinxiang 453007, China

c. State Key Laboratory of Urban Water Resource and Environment, School of Chemistry and Chemical Engineering, Harbin Institute of Technology, Harbin 150001, China.

d. MIIT Key Laboratory of Critical Materials Technology for New Energy Conversion and Storage, School of Chemistry and Chemical Engineering, Harbin Institute of Technology, Harbin 150001, Heilongjiang, China.

E-mail address: *esguili@scut.edu.cn* (L. Li); *zhaodengke@htu.edu.cn* (D. Zhao); *mzan@hit.edu.cn* (M. An)

1. Experimental Section

1.1. Materials

Cobalt nitrate hexahydrate ($Co(NO_3)_2 \cdot 6H_2O$, 98%), trisodium citrate, potassium ferricyanide ($K_3Fe(CN)_6$), sodium hypophosphite (NaH_2PO_2, 99%), potassium hydroxide (KOH), ammonia water ($NH_3 \cdot H_2O$), ethanol ($\geq$99.7%), dicyandiamide and Perfluorosulfonic acid-PTFE copolymer (Nafion solution, 5%) are purchased from Shanghai Aladdin Biochemical Technology Co, Ltd. The argon gases is supplied from Messer. Zinc plates and hydrophobic carbon paper are purchased from Alfa Aesar. All the reagents used in this experiment were obtained from commercial suppliers and directly used without any purification.

1.2. Synthesis of CoFePBA

In a typical synthetic procedure, 4 mmol of $K_3Fe(CN)_6$ is dissolved in 120 mL of DIW. Meanwhile, 6 mmol $Co(NO_3)_2 \cdot 6H_2O$ and 6mmol trisodium citrate are mixed in 120 mL of DIW. Then, these two solutions are mixed with vigorous stirring for 0.5h, and the mixed solution is aged at room temperature (25°C) for 48 h. The precipitate is collected by centrifugation, during which the impurities are removed several times by washing with deionized water and ethanol solution, and finally the collected precipitate is dried at 60°C overnight to obtain the CoFePBA nano cubes.

1.3. Synthesis of CNQDs

The g-C_3N_4 is prepared by the in situ copyrolysis method by dicyandiamide at 550°C for 4 h with a ramping rate of 2 °C min^{-1} thermal. Then, 0.534 g of the as-prepared g-C_3N_4 were dispersed in 30 mL $NH_3 \cdot H_2O$ (37wt%) stir well. Then the homogeneous solution is transferred into a 50 mL Teflon-lined autoclave, which is sealed and maintained at 150°C for 12 h. After the autoclave is cooled to room temperature (25°C), the resulting CNQDs intermixture is centrifuged at 8000 rpm for 15 min to remove any precipitate. Then, the obtained aminating g-C_3N_4 is collected supernatant to get the dispersed solution of the CNQDs.

1.4. Synthesis of CoFePBA@CNQD

CoFePBA (100 mg) is dispersed in 20 mL DIW and 20 mL of ethanol under vigorous stirring. Then, the dispersed CNQDs solution (4 mL) is added to the above solution, and the mixture is transferred into a 50 mL Teflon-lined autoclave. After heating at 180°C for 6 h, the CoFePBA@CNQD nanocubes are obtained by washing with DIW and drying at 60 °C under vacuum overnight.

In contrast, the samples with dispersal solutions of different substances (g-C_3N_4 and $NH_3 \cdot H_2O$) are synthesized using CoFePBA as the precursor and are named CoFePBA@g-C_3N_4 and CoFePBA@$NH_3 \cdot H_2O$, respectively.

1.5. Synthesis of a-CoFePO$_x$@CNQD

In the typical synthesis procedure, a-CoFePO$_x$@CNQD nanocages are synthesized using a low-temperature phosphating method. In 1:20 ratio of 20 mg CoFePBA@CNQD: 400 mg NaH_2PO_2 is placed at two separate positions in a porcelain boat with NaH_2PO_2 at the upstream side of the tube furnace. The sample is then annealed at 350°C for 2 h in a tube furnace at a heating rate of 2 °C min^{-1} under an Ar atmosphere. The a-CoFePO$_x$@CNQD nanocages are obtained after cooling to ambient temperature.

In contrast, a series of products are synthesized using different precursors (CoFePBA@g-C_3N_4 and CoFePBA@$NH_3 \cdot H_2O$). The above precursors are prepared with the same phosphating temperature and amount and are named a-CoFePO$_x$@g-C_3N_4 and a-CoFePO$_x$, respectively. Furthermore, in order to explore the effect of phosphating temperature, CoFePBA@CNQD is calcined at 300°C and 400°C, and named as a-CoFePO$_x$@CNQD-300，a-CoFePO$_x$@CNQD-350 and a-CoFePO$_x$@CNQD-400, respectively.

1.6. Materials characterization

The crystalline phase is determined by powder X-ray diffraction (XRD). Powder X-ray diffraction (XRD) patterns of Cu Ka radiated beams are measured with a Bruker

Foucs D8-Advance diffractometer. The scanning rate is 10° per min in 2θ with a scan range of 10-90°. The morphology and structure of the samples are characterized by the scanning electron microscope (SEM, S-4800, Hitachi). Transmission electron microscope (TEM) images are taken with a Tecnai G2-F20 at an accelerating voltage of 100 kV, energy-dispersive X-ray spectroscopy (EDS). X-ray photoelectron spectra (XPS) are used to confirm the chemical composition of the samples by a Phi X-tool instrument (Al Ka, 1486 eV), and the binding energy elements are calibrated by the C1s at 284.6eV. The N_2 adsorption- desorption isotherms are used to probe the specific surface area and pore size distribution of the samples by the Brunauer-Emmett-Teller (BET, ASAP 2010 instrument). Fourier transform infrared (FTIR) spectra were recorded by a Thermo Nicolet Nexus spectrometer.

1.7. Electrochemical measurements

The electrochemical measurements for the experiment are performed using a three-electrode system with an electrochemical workstation (CH Instruments, Model CHI 660E). The catalyst ink is prepared by sonication with 5 mg of catalyst is dispersed ultrasonically in a mixture of 940 μL ethanol, 40 μL DIW and 20 μL 5 wt% Nafion solution. In 1 M KOH solution, 5 mg of catalyst is used to form a homogeneous ink. The catalyst (with a loading of approximately 0.5 mg cm^{-2}) modified carbon cloth electrode, Ag/AgCl electrode and graphite rod are used as the working electrode, reference electrode and counter electrode, respectively. All potentials are corrected here with iR compensation by the formula $E = E_{test} - iR_s$ and calibrated to the RHE according to the conversion formula: $E_{RHE} = E_{Ag/AgCl} + 0.059pH + 0.197$ V. The linear scan voltammetry (LSV) measurements of the OER with a scan rate of 5 mV s^{-1} are tested from 1.0 to 1.8 V vs. RHE in a 1 M potassium hydroxide (KOH) solution. Fitting the linear part of the polarization curve with the following equation yields the corresponding Tafel diagram: $\eta = b \log(j) + a$, in which j is the current density and b is the Tafel slope. Electrochemical impedance spectroscopy (EIS) is obtained at an overpotential of 10 mAcm^{-2} current density with a frequency range from 100 kHz to 0.01 Hz. The electrochemical double-layer capacitance (C_{dl}) is detected by cyclic

voltammetry curves (CV) with different scan rates (40, 80, 120, 160 and 200 mV s^{-1}) at non-Faradaic potential (1.1-1.2 V vs. RHE for OER). The CV curves measured at different scan rates are fitted linearly to calculate the C_{dl}. The electrochemical specific area (ECSA) can be calculated by the following formula: ECSA = C_{dl}/60 μFcm^{-2}. Overall water-splitting measurements are tested with an electrochemical workstation (CHI 660) in a 1 M KOH electrolyte. The a-CoFePO$_x$@CNQD catalyst, applied to a carbon cloth substrate as the anode and the Pt/C catalyst is used as cathode, the load capacity is about 1 mg cm^{-2}. The LSV curves are obtained in the voltage range of 1.0 to 2.0 V. Additionally to the stability test i-t curve is measured at a voltage of 1.6 V.

1.8. Rechargeable Zn-air battery test

The Zn-air battery is assembled by a newly polished Zn plate with a thickness of 0.25 mm as the anode, a mixed aqueous solution is composed of 6.0 M KOH and 0.2 M Zn(Ac)$_2$ as the electrolyte, and the ink of the a-CoFePO$_x$@CNQD is loaded on a carbon cloth as the cathode. The catalyst ink is prepared as follows: 5mg a-CoFePO$_x$@CNQD is dispersed in 1 mL solution (20 μL nafion solution, 40 μL deionized water and 940 μL ethanol solution). As a comparison, the RuO$_2$+Pt/C ink is prepared by the same way, and then the same capacity of the RuO$_2$+Pt/C ink is loaded onto a carbon cloth. The battery discharge/charge performance and cycling reversibility are tested by the LANHE-CT2001A testing system by discharging and charging at 5 mA cm^{-2} with oxygen continuously fed to the cathode during the measurements. The voltage-current polarization curves are collected using the CHI 660E electrochemical workstation. Discharge power density is calculated the data from the discharge polarization curves according to the following equation: P = U_d × j_d, where P is the discharge power density, U_d is the discharge voltage, and j_d is the discharge current density.
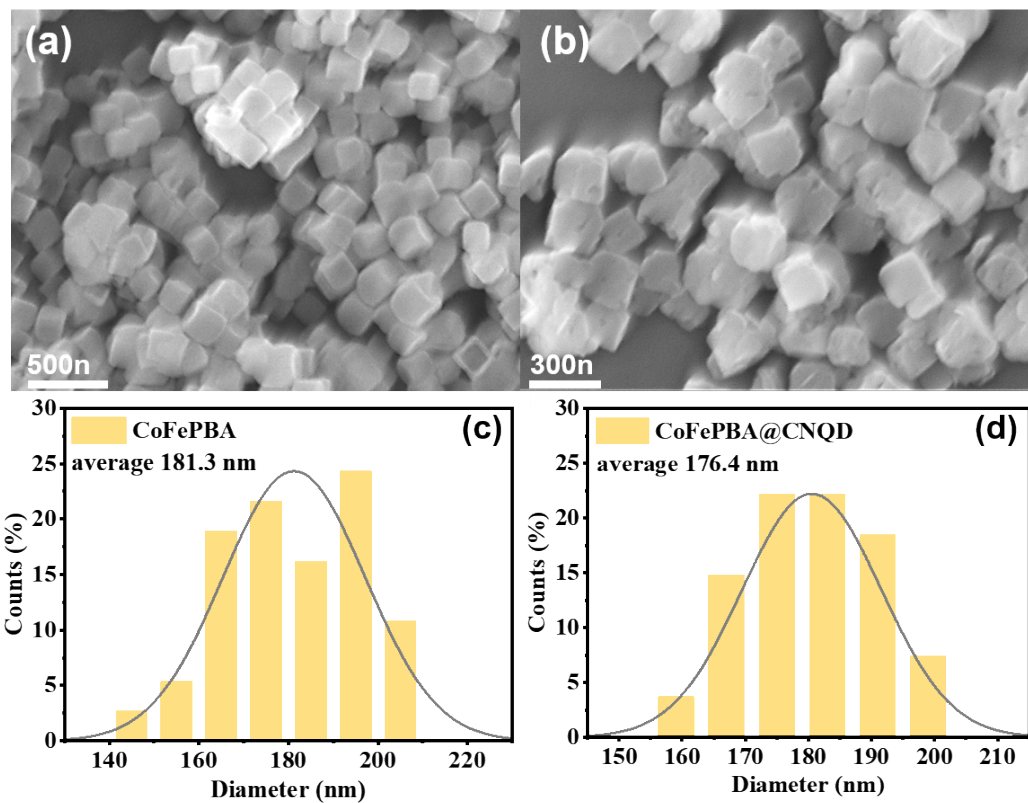
Figure S1. SEM image of (a) CoFePBA, (b) CoFePBA@CNQD. The statistical particle size distribution of (c) CoFePBA, (d) CoFePBA@CNQD.
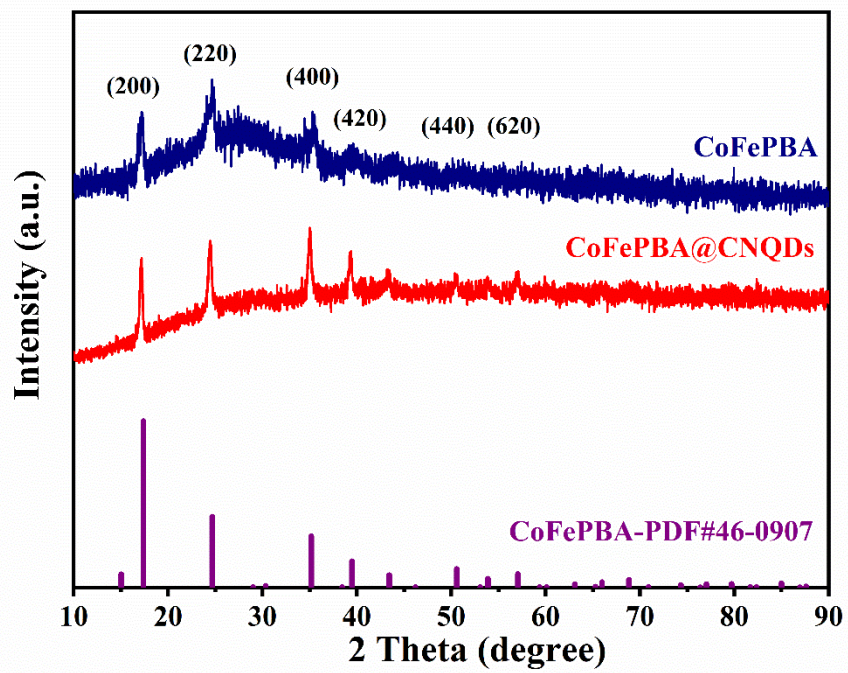
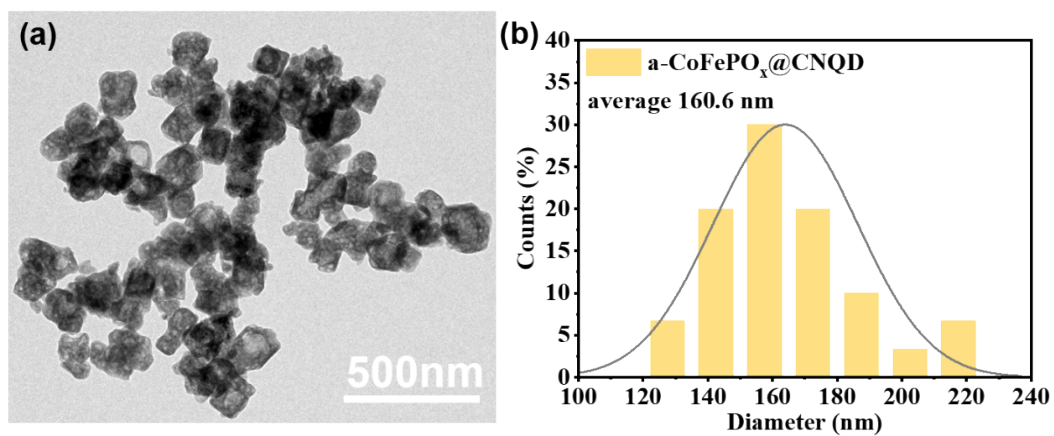**Figure S2.** XRD of CoFePBA and CoFePBA@CNQD.

Figure S3. (a)TEM image of a-CoFePO$_x$@CNQD, (b)The statistical particle size distribution of a-CoFePO$_x$@CNQD
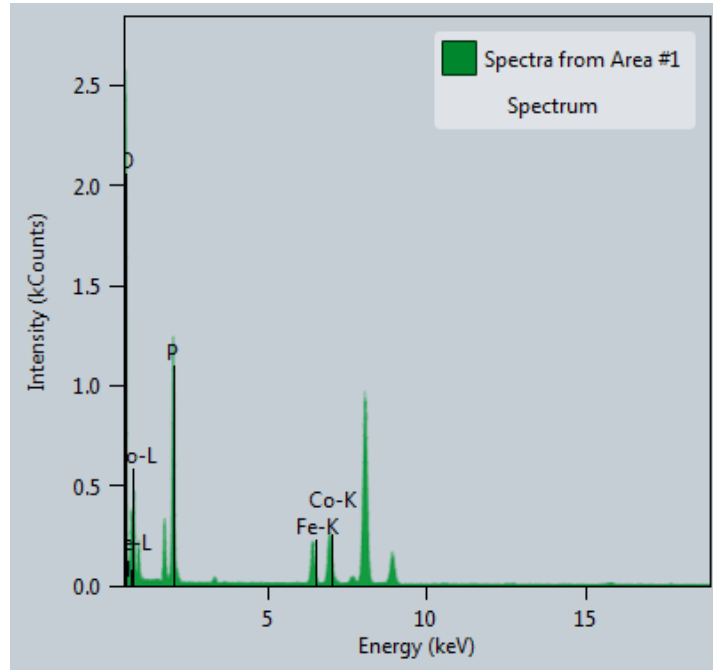
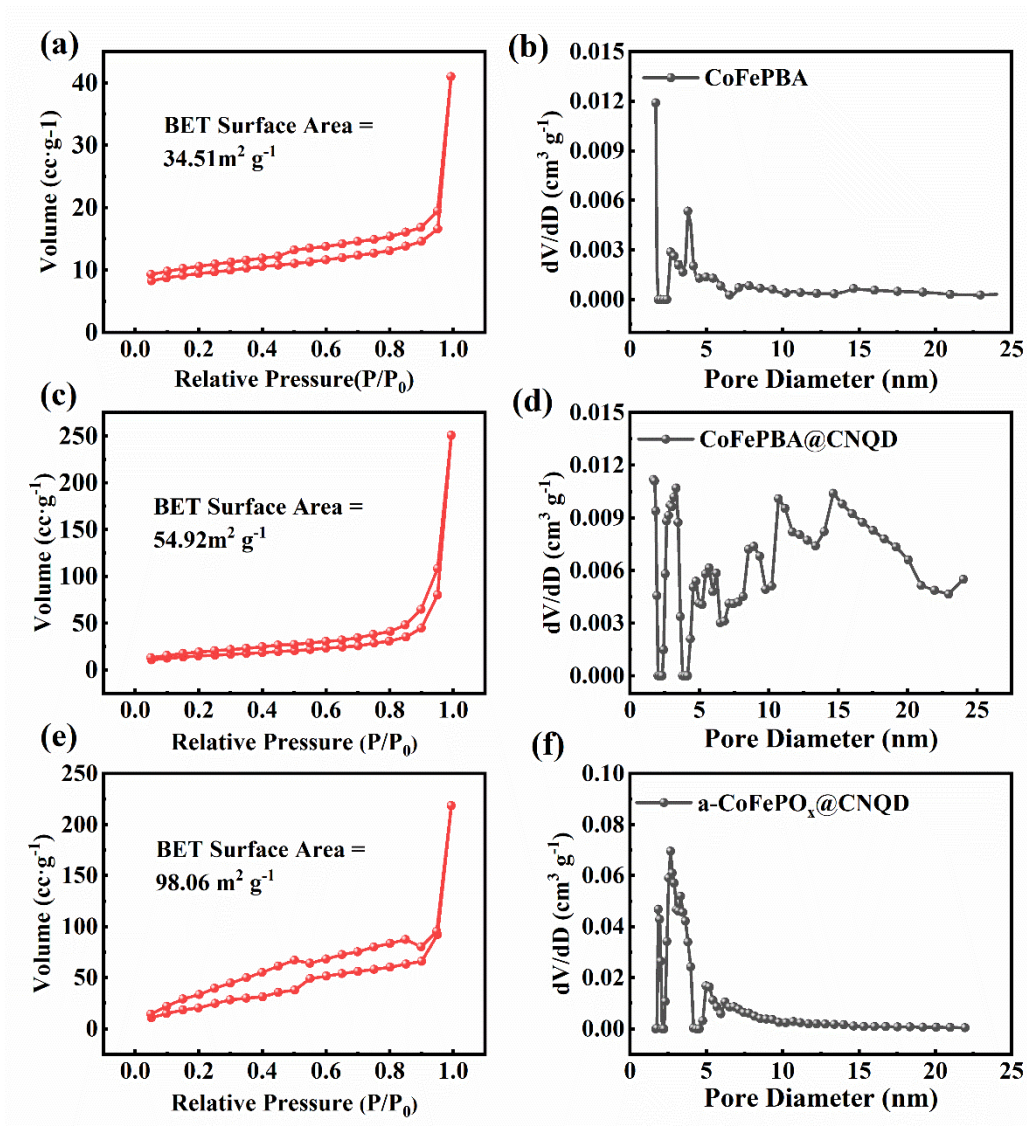**Figure S4.** The EDS spectrum of a-CoFePO$_x$@CNQD.

Figure S5. （a, c, e）Nitrogen adsorption-desorption isotherms of as-made samples.

(b, d, f) the corresponding pore-size distribution plots of as-made samples.
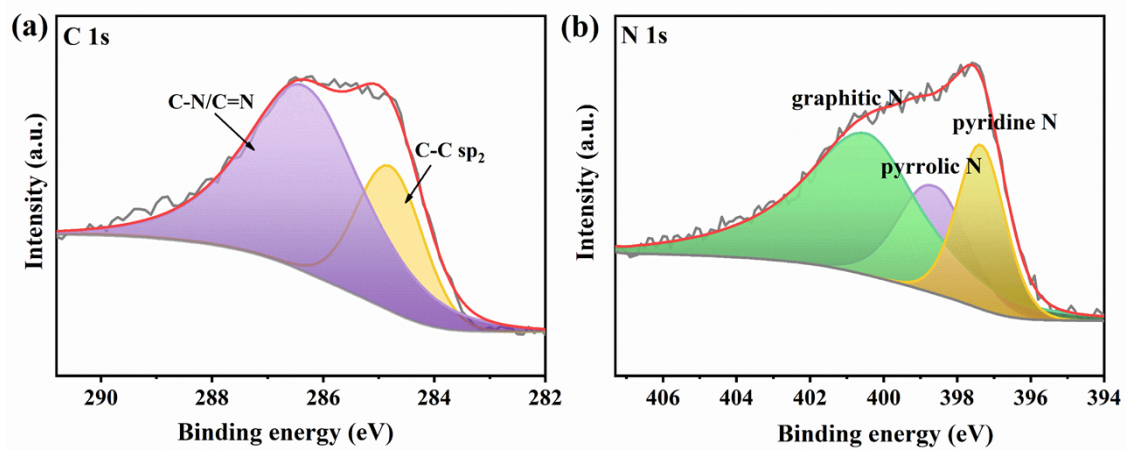
Figure S6. (a) high-resolution C 1s. (b) N 1s XPS spectrum of a-CoFePO$_x$.
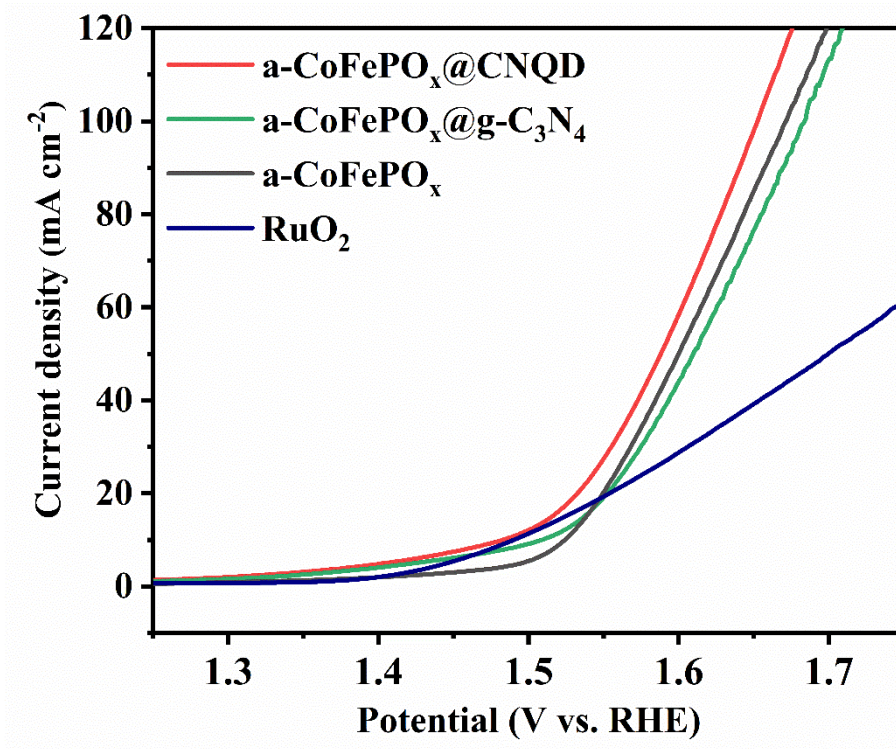
Figure S7. The LSVs without iR of different samples in 1.0 M KOH solution
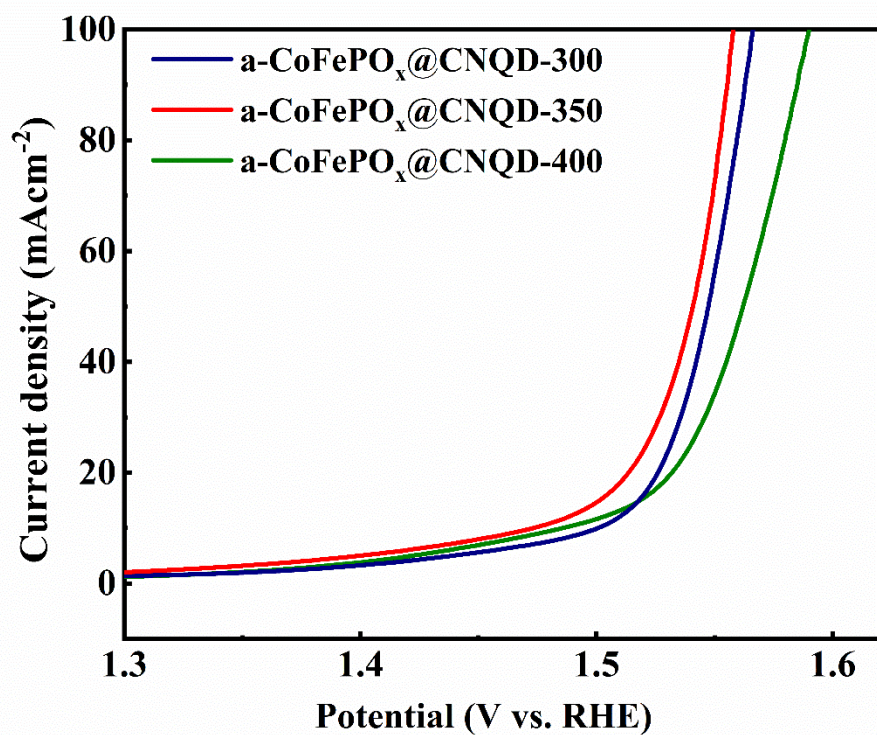
Figure S8. OER polarization curves of a-CoFePO$_x$@CNQD-300, a-CoFePO$_x$@CNQD-350, and a-CoFePO$_x$@CNQD-400 at a scan rate of 5 mV/s.
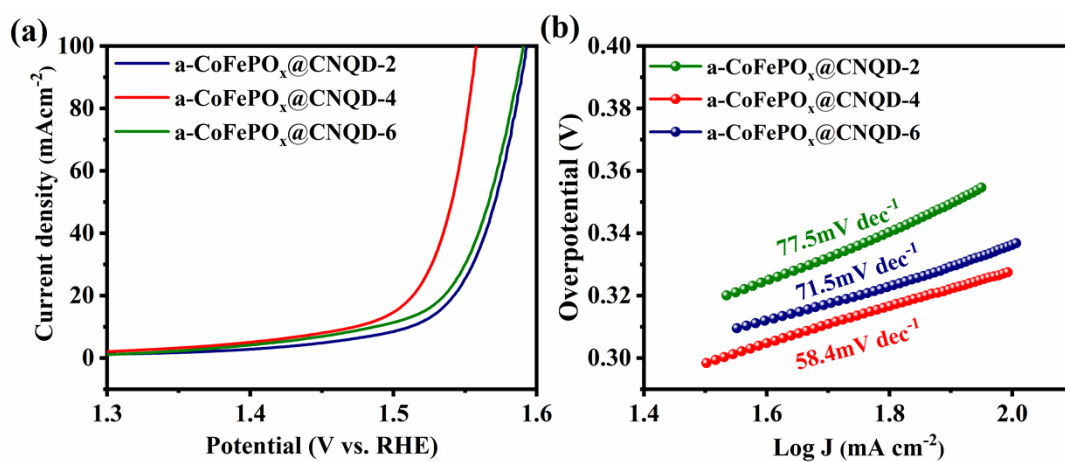
Figure S9. (a) LSV curves and (b) Tafel pots of CoFePO$_x$@CNQD-x (x = 2, 4 and 6) in 1 M KOH solution.
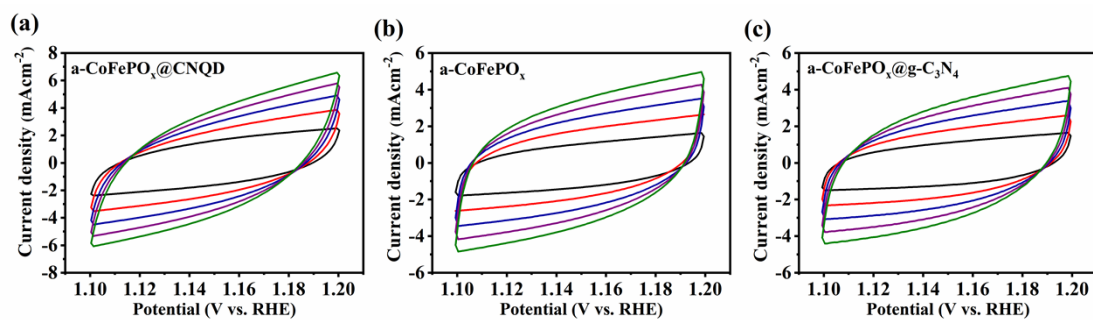
Figure S10. ECSA curves of the (a) a-CoFePO$_x$@CNQD, (b) a-CoFePO$_x$ and (c) a-CoFePO$_x$@g-C$_3$N$_4$, in 1.0 M KOH seawater under different scan rate in a region of 1.1 to 1.2 V vs RHE with different scan rate (40, 80, 120, 160 and 200 mV s^{-1}).
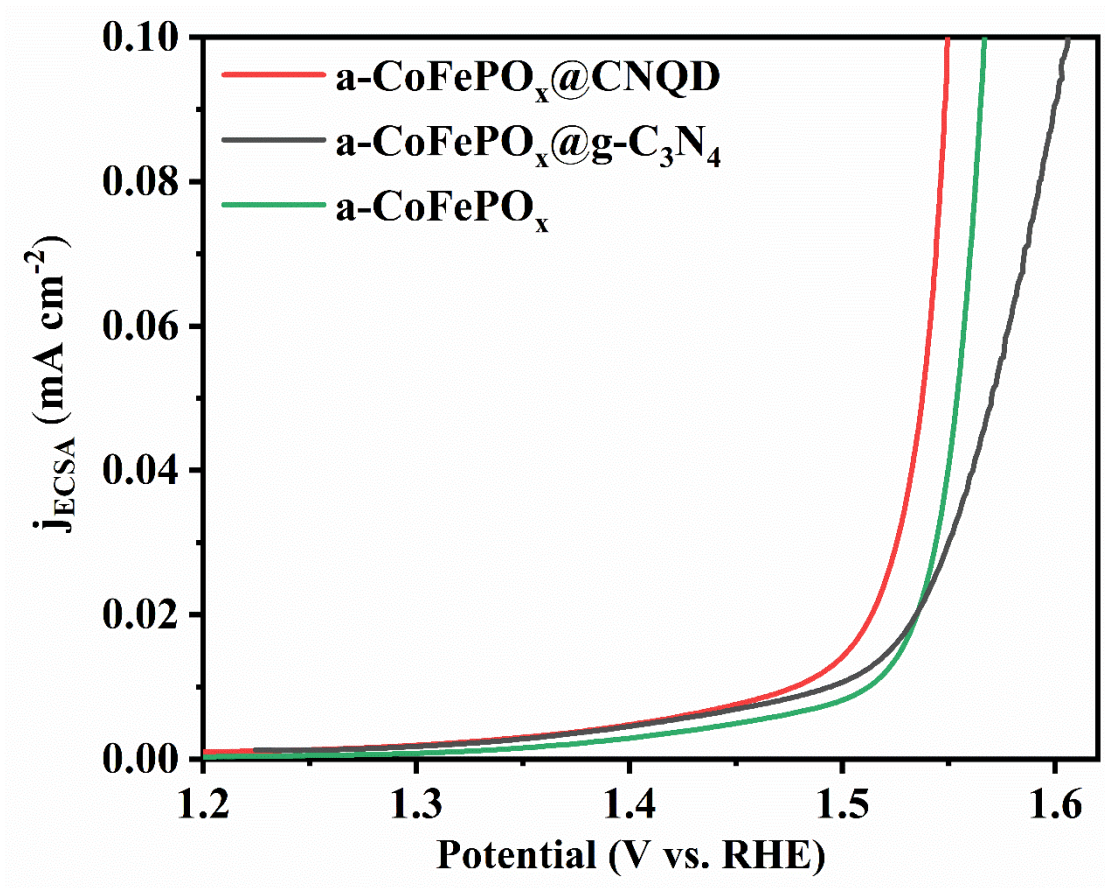
Figure S11. ECSA normalized OER polarization curves of a-CoFePO$_x$@CNQD, a-CoFePO$_x$@g-C$_3$N$_4$ and a-CoFePO$_x$.
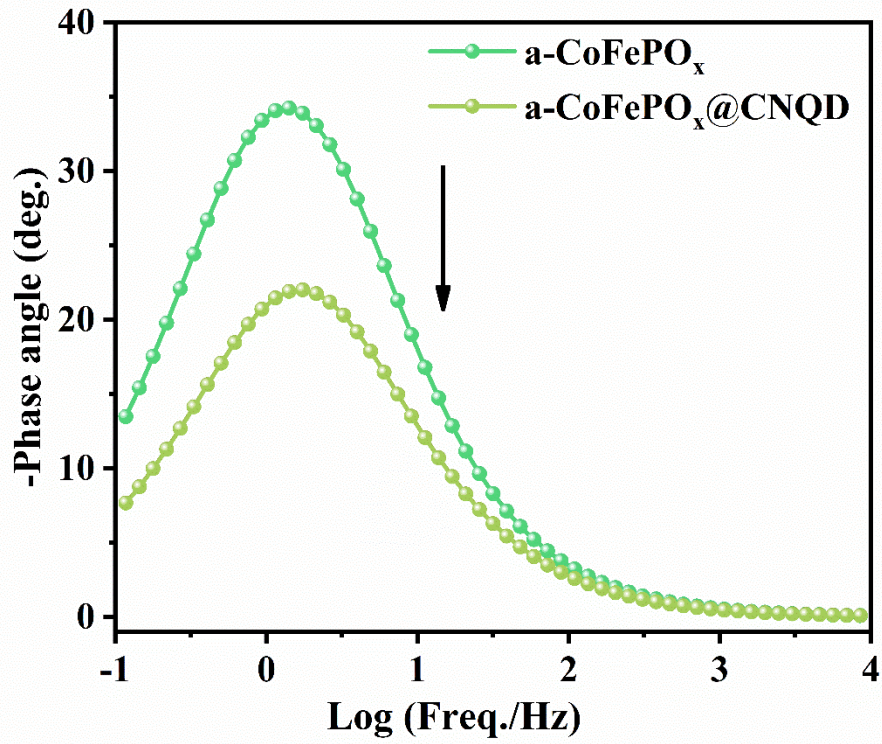
Figure S12. Bode plots of a-CoFePO$_x$@CNQD and a-CoFePO$_x$ for the OER at 0.45V versus Hg/HgO.
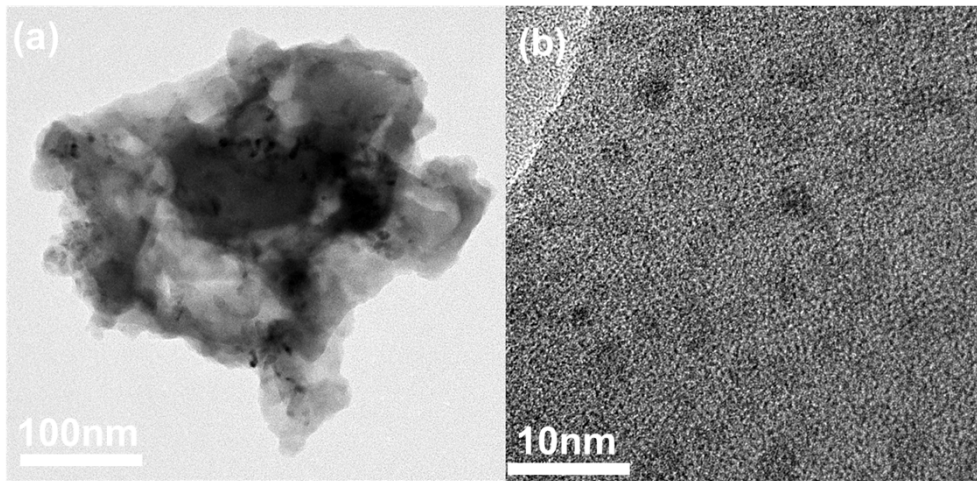
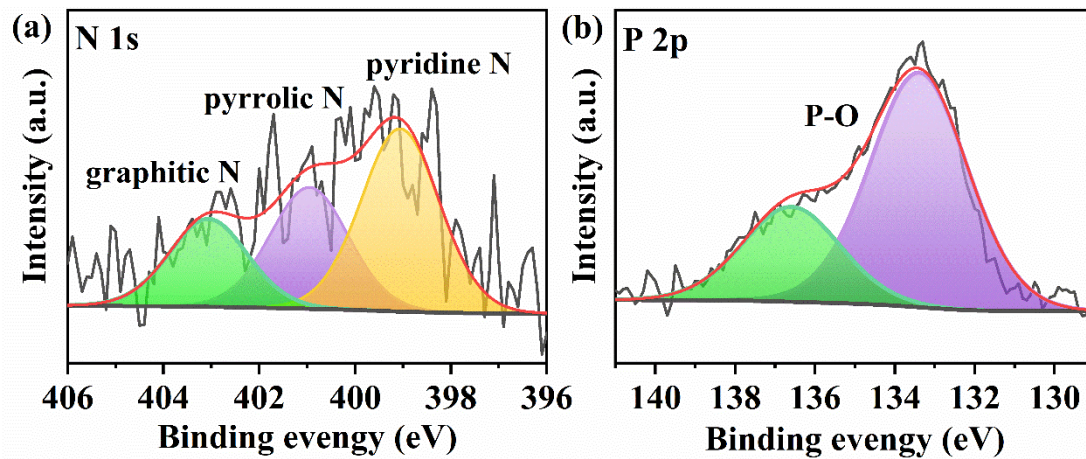**Figure S13.** (a, b) TEM images of a-CoFePO$_x$@CNQD after stability testing.

Figure S14. (a) high-resolution N 1s (b) P 2p XPS spectrum of a-CoFePO$_x$@CNQD after OER.
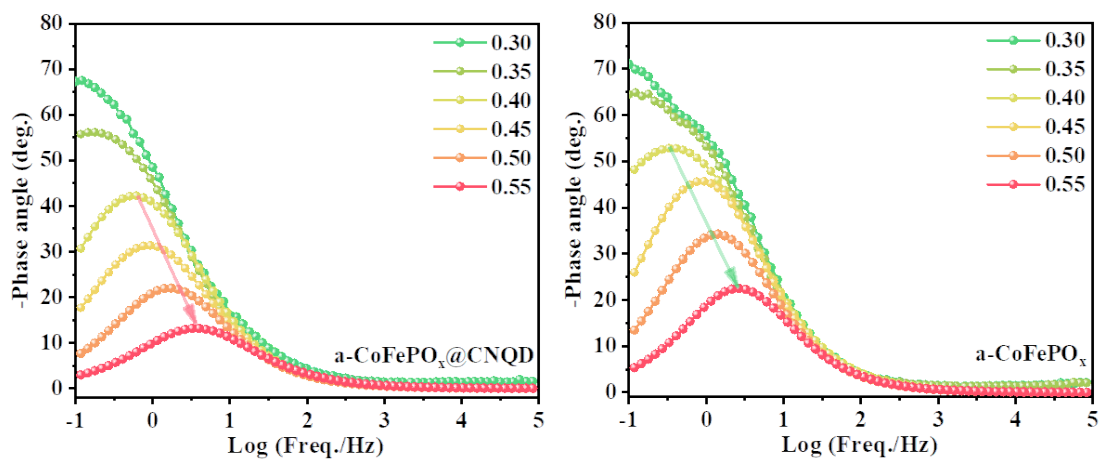
Figure S15. Bode plots of (a) a-CoFePO$_x$@CNQD and (b) a-CoFePO$_x$ for the MOR at different potentialsin 1 M KOH aqueous solution with 1 M MeOH.
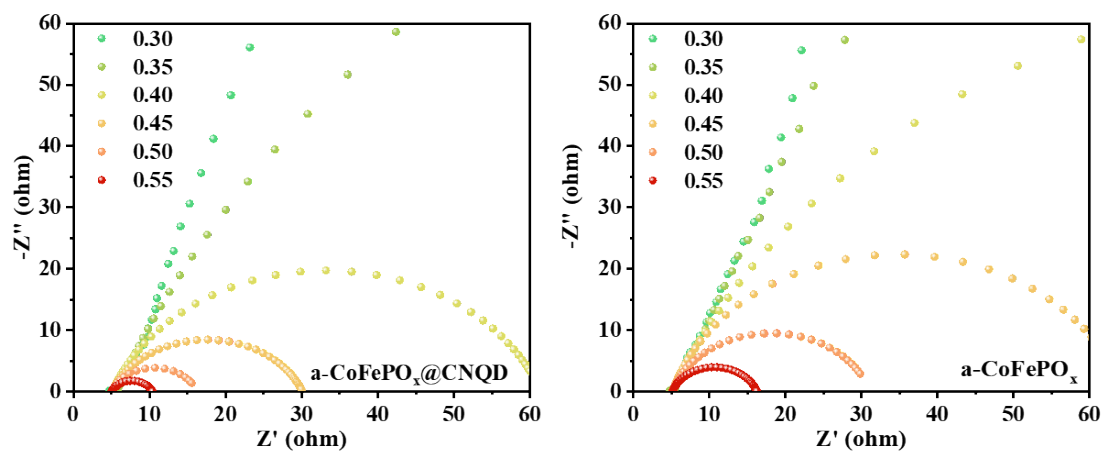
Figure S16. EIS Nyquist plots of (a) a-CoFePO$_x$@CNQD and (b) a-CoFePO$_x$ at different potentials versus Hg/HgO in 1 M KOH aqueous solution with 1 M MeOH.
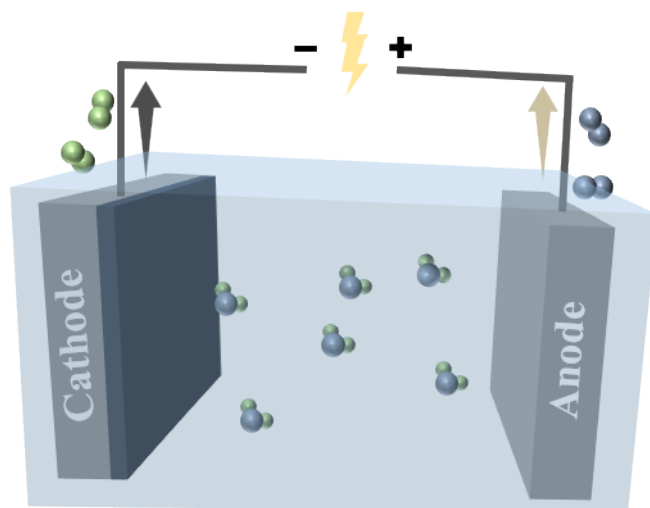
Figure S17. Schematic representation of the OWS.

Table S1. Element content of a-CoFePO$_x$@CNQD.

Element	Atomic Content (at. %)	Mass Content (wt. %)
C	44.51	30.82
N	2.37	2.29
O	35.47	30.65
Co	12.03	20.04
Fe	2.55	7.31
P	3.12	8.89

Table S2. Comparison of OWS performance in 1 M KOH (seawater) electrolyte between a-CoFePO$_x$@CNQD and reported bifunctional catalysts.

Catalysts	Voltage (V)	Ref.
a-CoFePO$_x$@CNQD	1.54	This work
CoFeP@C	1.56	[1]
FeNiP@C	1.71	[2]
FCNP@CQDs	1.61	[3]
a-Co(PO$_3$)$_2$/MoO$_4$/rGO	1.55	[4]
CoFeP@rGO	1.59	[5]
CoP NFs	1.65	[6]
FeCoNiP@NC/Ni	1.73	[7]
FeCoP arrays	1.60	[8]
Fe-doping CoP	1.68	[9]

Current density: 10 mA cm^{-2}

Electrolyte: 1 M KOH

References

1.   W. Li, Y. Chen, B. Yu, Y. Hu, X. Wang and D. Yang, *Nanoscale*, 2019, **11**, 17031-17040.

2.   Y. Song, S. Hu, X. Dong, Y. Wang, C. Wang and Y. Xia, *Electrochimica Acta*, 2014, **146**, 485-494.

3.   S. J. Lv, Y. Deng, Q. Liu, Z. Q. Fu, X. B. Liu, M. H. Wang, Z. Y. Xiao, B. Li and L. Wang, *Appl Catal B-Environ*, 2023, **326**.

4.   D. Zhao, S. Ning, X. Yu, Q. Wu, W. Zhou, J. Dan, Y. Zhu, H. Zhu, N. Wang and L. Li, *J Colloid Interface Sci*, 2022, **609**, 269-278.

5.   W. Li, B. Yu, Y. Hu, X. Wang, B. Wang, X. Zhang, D. Yang, Z. Wang and Y. Chen, *Journal of Power Sources*, 2020, **456**.

6.   L. Ji, J. Wang, X. Teng, T. J. Meyer and Z. Chen, *ACS Catalysis*, 2019, **10**, 412-419.

7.   J. R. Sun, S. S. Li, Q. Q. Zhang and J. Q. Guan, *Sustain Energ Fuels*, 2020, **4**, 4531-4537.

8.   L. Zhou, M. Shao, J. Li, S. Jiang, M. Wei and X. Duan, *Nano Energy*, 2017, **41**, 583-590.

9.   Q. Kang, M. Li, J. Shi, Q. Lu and F. Gao, *ACS Appl Mater Interfaces*, 2020, **12**, 19447-19456.